



Technology and Instrumentation in Particle Physics 2011

## BVIT: A visible imaging, photon counting instrument on the Southern African Large Telescope for high time resolution astronomy

Jason B. McPhate<sup>a,\*</sup>, Oswald H. W. Siegmund<sup>a</sup>, Barry Y. Welsh<sup>a</sup>, John V. Vallerga<sup>a</sup>, David A. H. Buckley<sup>b</sup>, Amanda A. S. Gulbis<sup>b</sup>, Janus D. Brink<sup>b</sup>, Doug Rogers<sup>a</sup>

<sup>a</sup> Space Sciences Laboratory, University of California, Berkeley, CA 94720 USA

<sup>b</sup> South African Astronomical Observatory, Observatory, 7935 South Africa

### Abstract

The Berkeley Visible Imaging Tube (BVIT) was installed on the Southern African Large Telescope (SALT) in January 2009 and subsequently refurbished in August 2010. BVIT is an imaging, photon counting camera with multi-color (B, V, R, and H- $\alpha$ ) capability. At the heart of BVIT is a 25 mm diameter active area, microchannel plate, sealed tube device with a visible photocathode and a cross-delay line readout. For each detected event the readout electronics record an X, Y position, an event pulse size (P), and an arrival time (T) — recorded with 25 ns precision. Post-acquisition processing of the X, Y, P, and T photon lists can be used to build images and light curves (to whatever sampling rate is supported by the signal to noise of the source as detected). The instrument design is presented as well as some examples of data acquired with the instrument on SALT.

© 2011 Published by Elsevier Ltd.

*Keywords:* visible, photon counting, imaging, high time resolution, SALT

### 1. Introduction

The Berkeley Visible Imaging Tube (BVIT) instrument was designed to perform high time resolution astronomy in the visible and near infrared. It originated as a simple imaging, photon counting and time-tagging detector system first used on the Nickel 1 m telescope at Lick Observatory in 2006 [1]. The success of this early incarnation prompted a redesign and rebuild of BVIT, adding filters and improved electronics. This incarnation of BVIT was installed on the Southern African Large Telescope (SALT) in January of 2009 and has since been refurbished with a more sensitive detector and faster computer. BVIT is due to become a facility instrument at SALT in early 2012. The design of BVIT as it is currently installed on SALT is presented as well as a few examples of light curves of astronomical objects acquired with BVIT.

\*Corresponding author: [mcphate@ssl.berkeley.edu](mailto:mcphate@ssl.berkeley.edu).



Fig. 1: The Southern African Large Telescope is located in the South African High Karoo desert near Sutherland. SALT is a 10 m-class, fixed zenith angle telescope with a spherical, multi-segmented primary mirror.

## 2. Instrumental description

SALT is located in the South African High Karoo desert (Fig 1a) near the town of Sutherland (specifically, at  $32.4^\circ$  S,  $20.8^\circ$  E, 1783 m). The telescope has an 11 m effective diameter, multi-segmented ( $91 \times 1$  m), spherical primary mirror (Fig 1b). SALT, built on the principle of the Hobby-Eberly Telescope at McDonald Observatory in Texas [2], operates with a fixed zenith angle of  $37^\circ$  and does not move during target tracking. The scientific instruments are housed in a prime focus payload structure that translates above the primary to track targets. Integral to the payload are optics for spherical aberration correction and field rotation.

### 2.1. BVIT commissioning

BVIT is a visible sensitive, photon counting, imaging system with integrated color and neutral density filters that was designed to carry out high time resolution astronomy (25 ns precision) of variable objects. At the heart of BVIT is a visible sensitive, photon counting, imaging sealed tube with time tagging read-out electronics. Its imaging capability allows for simultaneous acquisition of target, sky background, and field/comparison stars. Because BVIT is a photon counting instrument acquired data can be corrected post-facto for a number of observing maladies, such as, variable seeing/focus, tracking drift, telescope vignetting. Furthermore, during post-observation data processing light curve binning can be chosen as finely as is supported by the signal to noise of the source. This flexibility is useful with highly variable sources. If a source flares during an observation, the derived light curve is not constrained to time bins determined by a pre-observation selected acquisition cadence, but can be optimally binned post-facto.

BVIT was installed in the Auxiliary bay of the SALT prime focus payload and commissioned in early 2009. The effective beam from the telescope at BVIT is  $f/4.2$ , resulting in a plate scale of  $220 \text{ arcsec}/\mu\text{m}$ , so the 25 mm diameter active area of the detector equates to a 1.9 arcmin field of view. Good seeing for the SALT site results in  $\sim 0.5 \text{ arcsec}$  resolution, with typical values roughly twice this [3]. So typical stellar spot sizes on the detector are significantly larger than the detector resolution (see Sec. 2.3). Immediately after BVIT commissioning and initial science observations SALT was taken off-line for upgrades, principally improvements to the spherical aberration corrector, from April 2009 through August 2010 [4]. During this SALT upgrade the prime focus payload was removed from the telescope, allowing easier access to BVIT. This access was taken advantage of to refurbish BVIT. In August 2010, the original detector was replaced

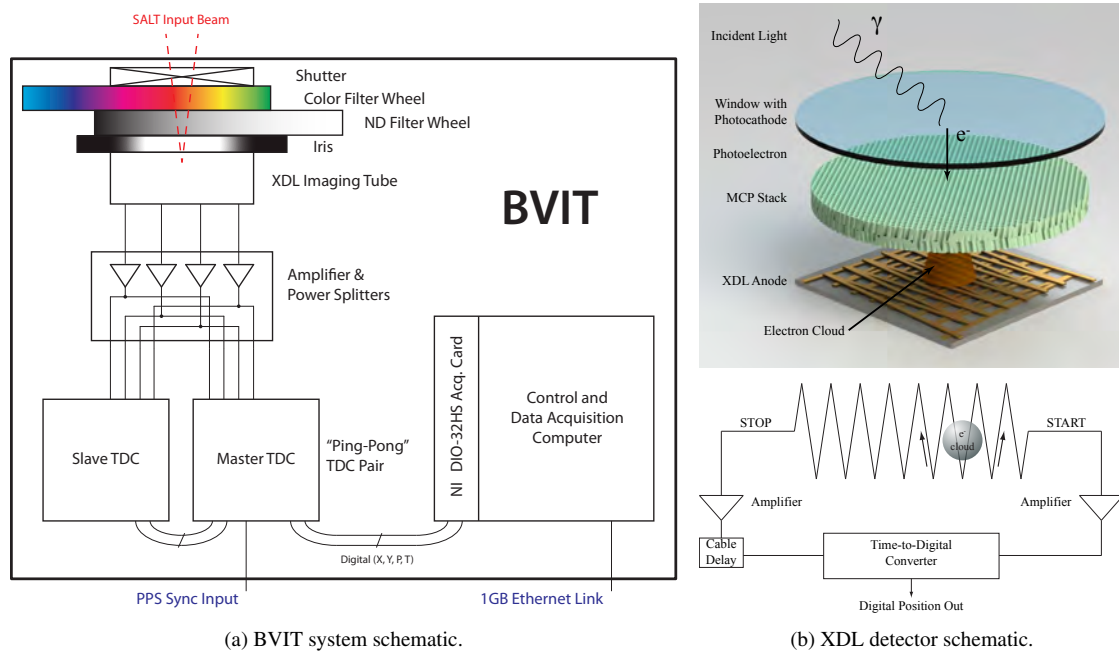


Fig. 2: Schematics of the BVIT instrument (a), the XDL detector (b-top) and one dimension of the XDL readout (b-bottom). Light entering BVIT from SALT passes sequentially through a shutter, a color filter wheel, a neutral density filter wheel, and a field stop iris before landing on the XDL imaging tube. The XDL tube converts incident photons into electrons and amplifies these via an MCP stack. The signals collected by the XDL detector are amplified and converted into image position via downstream time-to-digital electronics (with an X and Y position, charge size, P, and arrival time, T, recorded for each photon) and then passed to an on-board computer for later transfer to the control room.

with a more sensitive tube, with a SuperGen II photocathode, and a higher counting rate capability. The on-board computer was also exchanged for a faster one to keep up with the increased data rate. To reduce the thermionic detector background associated with the more sensitive photocathode and increased heat load of the more powerful CPU, an internal cooling loop was added. BVIT was back on the sky in December 2010, but shutter problems prohibited full science operations. The shutter was replaced and full science operations were again enabled in June 2011, including coordinated observations with the Rossi X-ray Timing Explorer satellite.

## 2.2. BVIT description

A schematic diagram of the BVIT instrument is shown in Fig 2a and a photograph of the inside of the instrument with the subcomponents labeled is shown in Fig 3a. Light from the telescope enters the BVIT enclosure and passes sequentially through a shutter, a color filter wheel, a neutral density filter wheel, and an adjustable iris – before reaching the imaging tube. Each filter wheel has five positions, one of which is left open (no filter). The color filter wheel positions are open and B, V, R, and H- $\alpha$  filters; the neutral density filter wheel positions are open and ND 0.3, ND 1, ND 3, and ND 4 filters. Filter wheels and color filters were purchased from Finger Lakes Instrumentation [5], neutral density filters were purchased from Andover, Inc. [6], and the H- $\alpha$  filter was purchased from Astronomik [7]. Filter transmissions are plotted in Fig 4b. The iris acts as a field stop, allowing the total sky background to be reduced if the source and comparison star are close enough to allow a reduction of the detector effective diameter.

A schematic representation of the imaging tube, which is at the heart of BVIT, is shown in Fig 2b and a photograph of the tube installed during the 2010 refurbishment is shown in Fig 3a. Photons landing on the

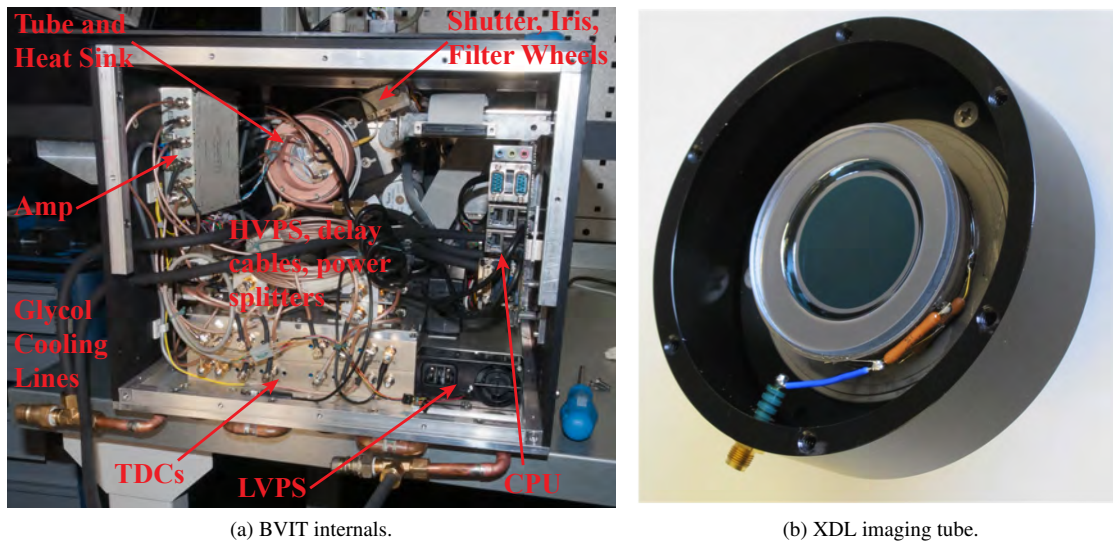


Fig. 3: (a) Photograph of the interior of the BVIT instrument with sub-components labeled. (b) The XDL imaging tube installed in BVIT in August 2010.

detector are converted to electrons by the photocathode. These photoelectrons are amplified (typical gains are  $10^6$  to  $10^7$ ) by a “Z” stack of three microchannel plates (MCPs) and collected by the cross delay line (XDL) anode. Image position is determined by the relative arrival times of the pulse at opposite ends of the delay lines. Signals from the XDL anode are amplified and passed to two time to digital converters (TDCs) for position encoding and time stamping. The TDCs accept input alternately, in a “ping-pong” scheme, to reduce electronic dead time. When one TDC receives a count it passes control to the other TDC, and vice versa.

The TDCs calculate the X, Y position of each event, as well as the MCP pulse size (P) and arrival time (T) in units of 25 ns clock cycles since the last sync signal. An external sync signal resets the TDC counters once per second to keep clock drift to a minimum. The X, Y, P, and T for each count is passed to the on-board computer (via a National Instruments DIO-32HS acquisition card). The custom data acquisition software uses a double memory buffer system to minimize data loss while writing to disk — while data from one buffer is being written to file, arriving data is stored in the other buffer. Data is stored on an on-board 500 GB hard drive. Each count requires 10 bytes of storage space. Data rates to the hard drive are limited to about 1.1 MHz; above this rate, data is lost at transitions between buffer writes. At the end of the night, all the data from the evening is downloaded from the instrument through a 1 GB Ethernet connection. Total power consumption is  $\sim 64$  watts, dominated by the TDCs, computer, and low voltage power supply (LVPS). This heat is removed via glycol-water heat exchangers (visible in Fig 3a) on the bottom of the instrument (for the TDCs and LVPS), on the tube, and on the CPU. The glycol-water cooling is provided by the SALT facility and is maintained at  $2^\circ\text{C}$  below the ambient temperature, to prevent condensation.

### 2.3. XDL imaging tube performance

The BVIT detector is a sealed tube, imaging, photon counting device. It has a proximity-focused, semi-transparent photocathode deposited on a reentrant window and a 25 mm diameter active area. Photoelectron amplification is performed by a “Z”-stack configuration of three MCPs with  $10\ \mu\text{m}$  pores diameters and 60:1 length to diameter ratio. The charge pulses emitted from the MCPs are collected with an XDL anode and the signals are further amplified before being sent to the TDCs. A single high voltage is applied to the tube, with the distribution between the photocathode gap, MCPs, and anode gap determined by a resistive bridge (one leg of which is the MCP resistance), see Fig 3b.

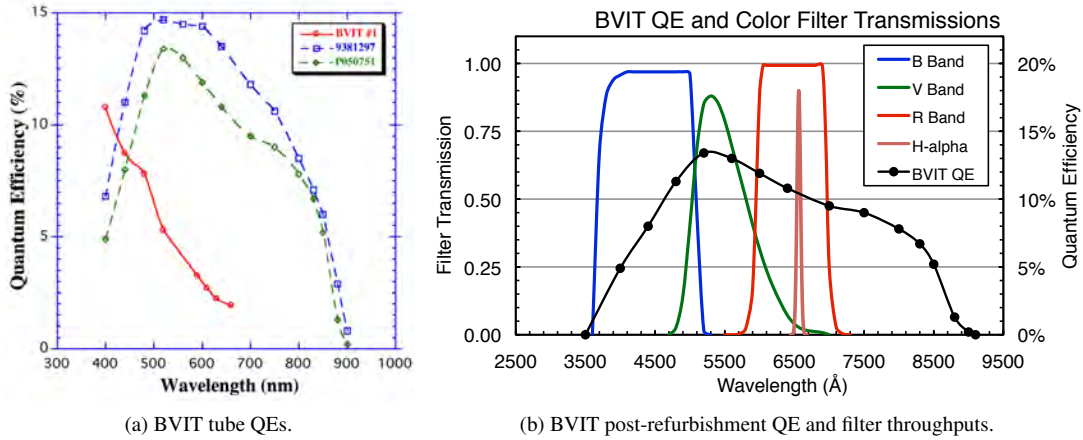


Fig. 4: (a) QES for the originally installed tube (red circles), replacement tube (green diamonds), and a spare (blue squares) that was deselected due to high background rate (see text for details). (b) Color filter throughputs and tube QE post refurbishment.

The tube originally installed in BVIT was produced at the University of California, Berkeley Space Sciences Laboratory and had an S20 multi-alkali photocathode. The photocathode quantum efficiency (QE) of this tube is plotted as the red curve (circles) in Fig 4a — it was sensitive in the blue and ultraviolet, but had poor red response. During the period of the SALT upgrades two new tubes were fabricated from Photonis/DEP ((Netherlands) with S25 (SuperGen II) multi-alkali photocathodes. The QEs of these tubes are shown as the green (diamonds) and blue (squares) curves in Fig 4a. One tube (blue curve) had higher QE but also had a higher background rate (~60 kcps), and so was selected against for this application. In August 2010 the other Photonis tube (green curve in Fig 4a and black curve in Fig 4b) was installed in BVIT. The photocathode background rate is temperature dependent, so internal cooling lines were added to cool the tube and extract heat from the CPU. In operation on the telescope, background rates have been in the 5–10 kcps range.

Given the tube QE and filter throughputs in Fig 4b and the effective collection area of SALT, the expected counting rates from 15<sup>th</sup> and 18<sup>th</sup> magnitude, spectrally flat sources are given in Table 1 for each color filter. While the detector and electronics can run at >2 Mcps, the global count rate is limited to ~1 Mcps by the computers ability to write data to hard drive. On nights with brighter sky background, the dominant contribution to the counting rate, decreasing the iris can help to reduce the global counting rate while using less ND to maximize source signal. To avoid detector burn-in and excessive local gain sag, sources brighter than ~100 kcps should not be observed without use of special observing techniques, for example, defocusing the image to spread the signal over a larger area, or lowering tube high voltage to decrease the average gain extraction per count. This source rate corresponds to a signal to noise ratio of 3 in 100  $\mu$ s. Ultimately, the system sensitivity and the local counting rate limits restrict observations to targets with  $12.5 < V_{\text{mag}} < 21.0$ .

The detector imaging spatial resolution and linearity were tested by projecting a rectilinear array of 10  $\mu$ m diameter pinholes (from a photo-lithographically deposited mask) onto the photocathode and characterizing the detector response (Fig 5a). The spatial resolution of the detector was characterized as a function

Table 1: Expected source counting rates (counts per second) for different BVIT color filter observing modes for 15<sup>th</sup> and 18<sup>th</sup> magnitude flat spectral sources. No neutral density filter is assumed.

| Filter      | $m = 15$ | $m = 18$ |
|-------------|----------|----------|
| B-band      | 57,000   | 3,600    |
| V-band      | 35,000   | 2,200    |
| R-band      | 28,000   | 1,800    |
| H- $\alpha$ | 1,600    | 100      |
| Open        | 150,000  | 10,000   |

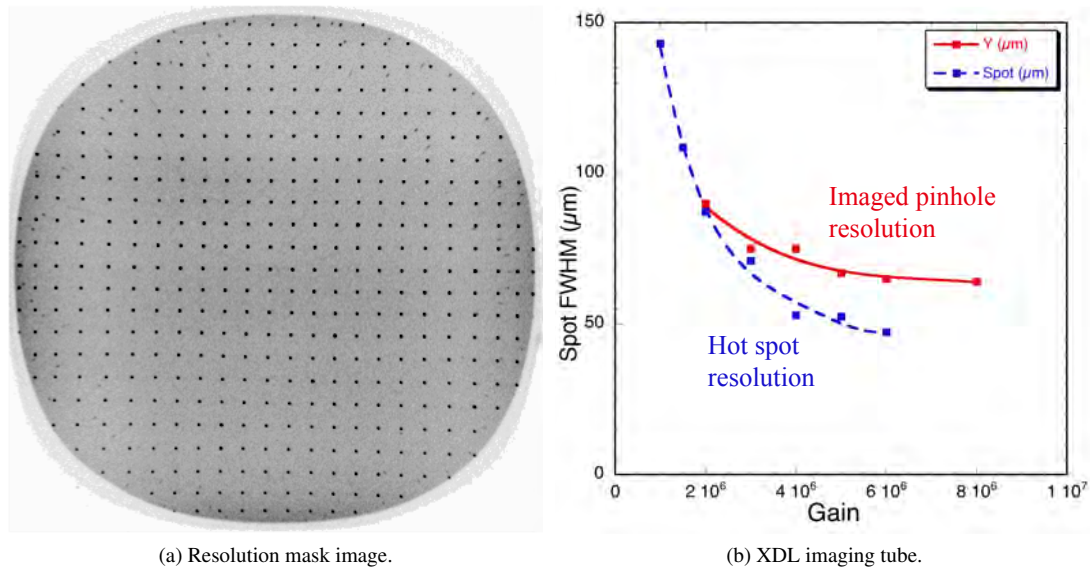


Fig. 5: (a) An image of a resolution mask taken with the BVIT imaging tube, each pinhole is  $10 \mu\text{m}$  as projected at the photocathode. (b) Tube resolution versus gain for the projected spots (as in a) and for a hot spot on the MCP surface. The resolution of the spots is degraded relative to the hot spot due to spreading of the electrons emitted by the photocathode prior to striking the MCP.

of MCP gain (solid, red line in Fig 5b) and, as is typical of these types of devices, gets better with increased gain until reaching an asymptotic resolution of  $\sim 80 \mu\text{m}$  at approximately  $4\text{--}5 \times 10^6$  gain. The dashed, blue line in Fig 5b is the spatial resolution of a hot spot on the MCP, showing that the dominant contribution to the detector resolution at gains above  $2 \times 10^6$  is caused by the photoelectron distribution spreading across the photocathode–MCP gap. Even so, the detector resolution is well below the typical  $200 \mu\text{m}$  stellar spot size coming from the telescope, allowing for quite a bit of latitude in lowering the detector gain without losing effective resolution. Operation at lower gain allows higher local counting rates and extends the lifetime of the tube.

### 3. Science observations

One of the most powerful aspects of an imaging, time-tagging, photon counting system like BVIT is the ability to post-process the data at whatever time scale is supported by the signal to noise ratio of the source, while simultaneously performing background and comparison star corrections. Two examples of light curves derived by temporally binning all the source counts collected on an object are displayed in Fig 6. Targets of interest include flare stars, eclipsing CV systems, low-mass X-ray binary systems, exoplanet transits, RRATs, and optical pulsars.

A light curve for a full eclipse of the  $18^{\text{th}}$  magnitude eclipsing binary cataclysmic variable system UZ Fornacis acquired in January of 2009 [8] is plotted in Fig 6a. The data is in counts per 500 ms bin. Material from the secondary, M-type star in this system is accreting onto the primary white dwarf, but only at the magnetic poles. The interesting two step profiles of the eclipse ingress and egress are due to the nature of how the hot accretion spots on the white dwarf are obscured by the inclined orbit of the companion M-type star. The data acquired with BVIT is at higher time resolution than previously measured on this source and allows better characterization of these shoulder features.

The 100 ms time bin light curve of a flare observed in January 2009 from the M-type flare star CN Leo [9] is plotted in Fig 6b. Note the small precursor and the significant structure in the main flare. Data such as

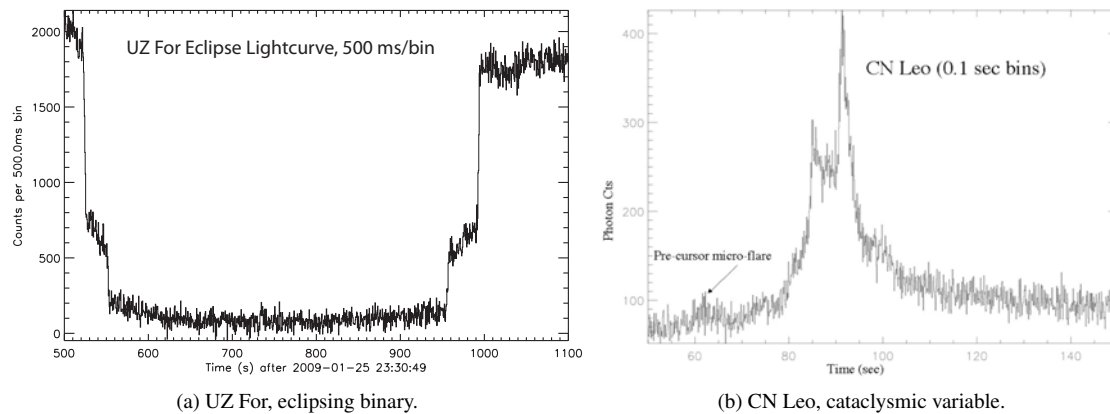


Fig. 6: (a) A light curve for the eclipsing binary system UZ For created using 500 ms time bins. (b) A light curve for the flare star CN Leo created using 100 ms time bins. Both light curves have been background and comparison star corrected (to remove telescope vignetting).

these are important for determining if micro-flares (such as these) are important heating mechanisms for the coronae of stars like our Sun. Resolving this question requires time resolution below 1 second.

We have also made serendipitous observations of other rapidly varying phenomena in the night sky, e.g. meteors transiting through the telescope field of view [10]. These can have transit times of several milliseconds across the BVIT  $\sim 2$  arcmin field of view. These transients mimic rapid variations in the light curve of a source if they pass by closely on the sky. The only way to be certain the source light curve is not contaminated by such a feature is to make an image of the transient or make a movie of time period in question.

#### 4. Future plans

BVIT will be turned into a user facility instrument at SALT in early 2012. This move is motivating a desire to have an improved user interface that is integrated more completely with the data acquisition software (these are currently two independently running pieces of software). Also a portable data extraction pipeline for users will need to be created. This task is currently being performed by a suite of programs running in the IDL language.

Possible improvements for a second generation BVIT instrument include the following: Improved sensitivity by use of a tube with a GaAsP photocathode. Using a cross-strip anode readout, which allows operation at lower gain and higher counting rates. Designing and employing custom readout electronics that would be smaller and lower power consumption. Using a better optical design with either a grism or simultaneous multi-color capability. And certainly a computer system with faster write to disk speeds to keep up with the increased data rates.

#### Acknowledgments

The authors are indebted to the engineering and IT staff at SALT for many hours of support without which the success of BVIT would not be possible. This includes (but is not limited to) Ockert Strydom, Charl Du Plessis, Hamish Whittal, Simon Fishley, Garith Dugmore, Eben Wiid, Peter Menzies, and Ardisha Pancham.

We would like to thank the following students and staff at UC Berkeley who worked on the design of BVIT and subsequent data processing: Rahul Barwani, Mike Quinones, Johathan Wheatley, Navid Radnia, and David Anderson.

This work was supported by NSF grants AST-0352980 and DBI-0552-099 to the University of California, Berkeley.

## References

- [1] O. H. W. Siegmund, J. McPhate, A. Tremsin, J. V. Vallergera, B. Y. Welsh, J. M. Wheatley, High time resolution astronomical observations with the Berkeley visible image tube, AIP Conference Proceedings 984 (1) (2008) 103–114.  
URL <http://link.aip.org/link/?APC/984/103/1>
- [2] R. Stobie, J. G. Meiring, D. A. H. Buckley, Design of the Southern African Large Telescope (SALT), Proc. SPIE 4003 (1) (2000) 355–362.  
URL <http://dx.doi.org/10.1117/12.391525>
- [3] J. G. Meiring, D. A. H. Buckley, Southern African Large Telescope (SALT) project progress and status after four years, Proc. SPIE 5489 (1) (2004) 592–602.  
URL <http://dx.doi.org/10.1117/12.551344>
- [4] D. A. H. Buckley, S. Crawford, A. A. S. Gulbis, J. McPhate, K. H. Nordsieck, S. B. Potter, D. O’Donoghue, O. H. W. Siegmund, P. Schellart, M. Spark, B. Y. Welsh, E. Zietsman, Time resolved astronomy with the SALT, Proc. SPIE 7735 (1) (2010) 773559.  
URL <http://dx.doi.org/10.1117/12.858039>
- [5] Finger Lakes Instrumentation webpage [cited 2011].  
URL <http://www.flicamera.com>
- [6] Andover Corporation webpage [cited 2011].  
URL <http://www.andovercorp.com/>
- [7] Astronomik webpage [cited 2011].  
URL <http://www.astronomik.com/en/>
- [8] S. B. Potter, E. Romero-Colmenero, G. Ramsay, S. Crawford, A. Gulbis, S. Barway, E. Zietsman, M. Kotze, D. A. H. Buckley, D. O’Donoghue, O. H. W. Siegmund, J. McPhate, B. Y. Welsh, J. Vallergera, Possible detection of two giant extrasolar planets orbiting the eclipsing polar UZ Fornacis, Mon. Not. R. Astron. Soc.  
URL <http://arxiv.org/abs/1106.1404v1>
- [9] O. Siegmund, J. Vallergera, B. Welsh, J. McPhate, A. Tremsin, High speed optical imaging photon counting microchannel plate detectors for astronomical and space sensing applications, AMOS Conference 2009.  
URL <http://www.amostech.com/technicalpapers/2009/poster/siegmund.pdf>
- [10] O. H. W. Siegmund, J. V. Vallergera, A. Tremsin, J. McPhate, B. Welsh, Optical photon counting imaging detectors with nanosecond time resolution for astronomy and night time sensing, AMOS Conference 2011.  
URL <http://www.amostech.com/TechnicalPapers/2011/Poster/SIEGMUND.pdf>